

Temperature-dependent transport properties of hydrogen-induced diamond surface conductive channels

J. A. Garrido, T. Heimbeck, and M. Stutzmann

Walter Schottky Institut, Technische Universität München, Am Coulombwall, D-85748 Garching, Germany

(Received 20 December 2004; published 13 June 2005)

Hall effect experiments have been carried out in diamond surface conductive channels induced by hydrogen termination. The conductivity and the Hall mobility have been studied as a function of temperature and carrier concentration. The conductivity and Hall mobility are exponentially activated with temperature, with almost identical activation energies, whereas the carrier concentration shows no or only a very weak temperature dependence, as expected for metallic conduction. The activation energy is found to decrease with increasing carrier concentration, until it almost vanishes. The experimental results are discussed in the frame of a model based on large-range potential fluctuations which give rise to metallic and insulating regions coexisting at the diamond surface. The conductivity and Hall mobility are analyzed using percolation theory. Below the percolation threshold, transport occurs by thermal excitation over the potential barriers separating the metallic regions. Above the percolation threshold, activated transport persists as the thermal emission over remaining potential barriers contributes to reduce the resistance of long percolating paths. The experimental results have been fitted using a model with three free parameters: metallic conductivity and mobility, averaged potential barrier, and surface fraction occupied by insulating regions. The Hall mobility in the metallic regions has been found to decrease with increasing carrier concentration, indicating a strong influence of surface scattering. The contribution of variable-range hopping at very low temperatures is also discussed.

DOI: 10.1103/PhysRevB.71.245310

PACS number(s): 73.25.+i, 72.20.Ee, 73.20.At

I. INTRODUCTION

The *p*-type surface conductive channel induced in hydrogen-terminated diamond surfaces is a very interesting system to study the effect of disorder-induced localization on the electronic transport properties of the accumulated holes. The combination of surface hydrogen termination and the presence of surface adsorbates produces the accumulation of holes in a surface channel,^{1,2} where carrier concentrations up to $5 \times 10^{13} \text{ cm}^{-2}$ have been reported.³ The holes are expected to form a two-dimensional channel in the close vicinity of the diamond surface, as a result of the strong electric fields perpendicular to the surface. Thus, the presence of charged surface adsorbates and structural defects is expected to play an important role for the transport and scattering of holes in the surface channel. Additionally, a laterally inhomogeneous hydrogen termination of the diamond surface should have a similar effect as the surface adsorbates. Therefore, noticeable surface potential fluctuations are expected, analogous to silicon inversion layers with interface oxide charges, which might give rise to carrier localization. Our main motivation is to advance the understanding of the transport properties of holes in conductive channels at the surface of hydrogen-terminated diamond, which still are not well understood. For instance, various works have reported a large dispersion in the values of the thermal activation energy of the conductivity.³⁻⁵ The activation energy has been reported to vary depending on the sample characteristics, as well as the atmosphere (He or vacuum) in which the experiment was done.³

In a previous paper,³ Nebel *et al.* have reported low-temperature Hall experiments performed on surface conductive diamond layers. The authors have demonstrated that the

transport characteristics of surface conductive diamond layers are governed by a narrow hole accumulation layer at the valence band edge where disorder-induced localized states are also present. Nebel *et al.* reported a critical temperature above which carriers are mobile in extended states and below which carriers are trapped in localized states. They assumed a classical mobility-edge model to explain their experimental results, suggesting that above the critical temperature, the transport mechanism resembles that of carriers moving in extended states.³

However, many Hall experiments carried out in Si/SiO₂ inversion layers with large density of interface charges, and therefore subjected to strong localization effects, have indicated that the transport properties in the studied temperature range cannot be described by the Anderson mobility-edge model.⁶⁻⁸ On the contrary, an “anomalous” Hall effect was reported, in which the conductivity and Hall mobility were thermally activated with the same activation energy, which varied with carrier concentration.^{9,10} Long-range potential fluctuations,⁹ hopping transport,¹¹ and correlation effects have been proposed to explain the experimental results.¹⁰

In this paper, we reconsider the transport properties of holes in two-dimensional (2D) conductive channels at the surface of hydrogen-terminated diamond samples. Low-temperature experiments have been carried out to understand the reported large dispersion of the activation energy of the conductivity. Moderately high-temperature annealing was used to vary the concentration of carriers in the conductive channel of the same sample, and to investigate its influence on the conductivity. Hall experiments have been performed to evaluate the impact of the expected surface disorder on the transport properties. In the studied temperature range (30–300 K), we did not observe freeze-out of carriers. On

the contrary, the conductivity and the Hall mobility show exponential activation, with almost the same activation energy. The activation energy increases with decreasing carrier concentration. Several models explaining this behavior are discussed. In view of the results we have adopted an early model by Arnold who, using percolation theory, attributed the activation of the conductivity and the Hall mobility to the presence of long-range inhomogeneities in the samples, suggesting that metallic and thermally activated conductivity co-exist over an appreciable range of carrier concentration.⁹

Our results have been fitted using the model proposed by Arnold with a very good agreement. However, at very low temperature our experimental results depart from the theoretical prediction, a behavior that is attributed to the influence of variable-range-hopping transport. Different parameters, such as activation energy, metallic conductivity, and density of disorder-induced states, are discussed in the text.

II. EXPERIMENT

Two different types of undoped diamond samples were used in order to evaluate the possible influence of the surface roughness on the transport properties. Synthetic type-IIa single-crystal diamond samples (both 100 and 111 oriented), with an average surface roughness below 1 nm, were used as examples of low-roughness surfaces. On the other hand, intrinsic polycrystalline chemical-vapor-deposited diamond samples with an average grain size of about 20–40 μm and about 50 μm of roughness were used to represent high-roughness surfaces. Prior to any process samples were cleaned in aqua regia at 150 °C for 1 h, to remove metal contamination at the surface. Then, the samples were chemically oxidized in two steps: first with a solution of $\text{CrO}_3/\text{H}_2\text{SO}_4$ at 150 °C for 1 h, and afterward in a mixture of $\text{H}_2\text{O}_2/\text{NH}_4\text{OH}$ at 150 °C for 1 h. In addition to the oxygen termination of the diamond surfaces, this chemical treatment is known to remove graphitic surface carbon. The oxidation process was evaluated using contact angle experiments, which confirmed the surface hydrophilicity after the oxidation. Surface conductivity was induced by exposing the diamond surfaces to hydrogen radicals generated by a hot-filament setup. H_2 (with a flux of 150 cubic centimeters per minute at STP) was introduced in a vacuum chamber (base pressure 10^{-6} mbar) and activated with two hot (1900 °C) tungsten wires. During the hydrogenation process the chamber pressure was fixed to 1.5 mbar. The samples were exposed to the hydrogen radicals for 30 min at a temperature of 700 °C. After hydrogen termination the samples were kept for one day under ambient atmospheric conditions in order to induce the surface conductivity. Contact angle experiments showed highly hydrophobic surfaces, in contrast to oxygen-terminated diamond.

The conductivity and Hall measurements were performed in vacuum (10^{-6} mbar) using Van der Pauw geometry. Magnetic fields of 1.8 T were applied for the Hall measurements. The samples were mounted in a cryostat where the temperature could be varied between 20 and 700 K without breaking the vacuum. In order to investigate the effect of the hole concentration on the transport properties, high-temperature

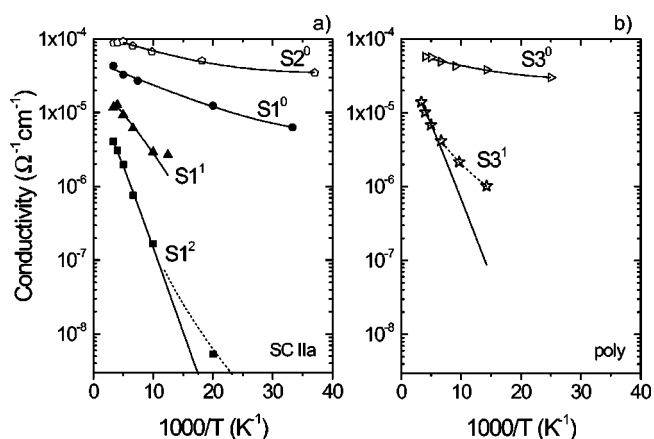


FIG. 1. Temperature dependence of the conductivity between 30 and 300 K. (a) Results measured in monocrystalline synthetic type-IIa samples (S1 and S3). (b) Results obtained for an undoped polycrystalline sample (S3). Open and solid symbols correspond to the experimental results. The upper index i in the label SX^i indicates that sample SX was annealed at high temperatures ($T \geq 500$ K) i times. Solid lines correspond to the calculation of the model described in the text, whereas dashed lines represent the contribution of variable-range hopping. Increasing the number of annealing steps results in a stronger temperature dependence of the conductivity.

annealing (500 K with variable time) was used to tune the desired hole concentration for each sample. At this annealing temperature, the C–H bonds are not expected to be affected,¹² but the number of holes accumulated inside the inversion layer is reduced because they are thermally excited out of the inversion channel. It has been shown that if the sample is kept in vacuum after annealing, carriers are not able to repopulate the channel.¹³

III. RESULTS

Figures 1(a) and 1(b) show the typical temperature-dependent conductivity for single-crystalline [Fig. 1(a)] and polycrystalline [Fig. 1(b)] surface conductive diamond samples. The symbols represent the experimental results, whereas the solid lines represent the conductivity calculated using a model which will be described in Sec. IV. In vacuum, and without any annealing process [corresponding to symbols in curves $S1^0$ and $S2^0$ in Fig. 1(a), and curve $S3^0$ in Fig. 1(b)], the measured conductivities at room temperature are in the range 5×10^{-5} – 10^{-4} $\Omega^{-1} \text{cm}^{-1}$, and decrease with decreasing temperature. However, the dependence of the conductivity with temperature is very weak for samples $S1^0$, $S2^0$, and $S3^0$. Moreover, at the lowest temperature the temperature dependence disappears as expected for the conduction of carriers in extended states of a 2D inversion layer. This is confirmed in Fig. 2, where the carrier concentration (extracted from Hall effect experiments) is shown to be almost independent of temperature. Annealing the samples in vacuum reduces the number of holes accumulated in the inversion layer, as shown in Fig. 2 for samples $S1$ and $S3$. For instance, in the case of sample $S1$ the carrier concentration (measured at room temperature) can be varied between 9

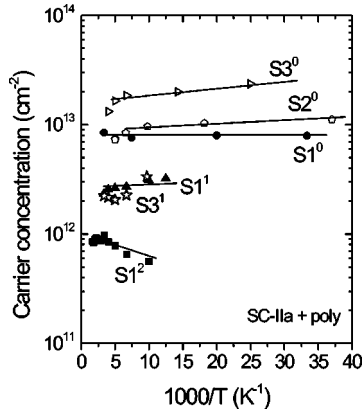


FIG. 2. Carrier concentration versus temperature measured by Hall experiments for different samples in different annealing states. The main effect of annealing is to reduce the carrier concentration, which can be tuned from 10^{12} to 10^{13} cm^{-2} at room temperature. In general, the carrier concentration shows only a weak temperature dependence.

$\times 10^{12}$ cm^{-2} for the nonannealed state ($S1^0$), 2.4×10^{12} cm^{-2} after one annealing step ($S1^1$), and 9×10^{11} cm^{-2} after two annealing steps ($S1^2$). A similar effect was also found in sample $S3$. The influence of the annealing process on the temperature dependence of the conductivity can be observed in Fig. 1. Reducing the number of carriers in the hole channel results in a stronger variation of the conductivity with temperature [curves $S1^1$ and $S1^2$ in Fig. 1(a), and curve $S3^1$ in Fig. 1(b)]. In the high-temperature regime, the temperature dependence of the conductivity resembles an exponentially activated behavior, with the activation energy increasing as the carrier concentration decreases. At lower temperatures the conductivity does not follow the pure exponential dependence with temperature. Interestingly, the activated behavior of the conductivity is not the result of an activated carrier concentration, as clearly seen in Fig. 2. Instead, the Hall mobility is temperature activated in a very similar way as the conductivity. Figures 3(a) and 3(b) show the temperature dependence of the Hall mobility for samples $S1$, $S2$, and $S3$. At room temperature and without any annealing the Hall mobility is in the range 30–100 $\text{cm}^2/\text{V s}$. Mirroring the behavior of the conductivity, at high temperature the mobility shows an exponentially activated behavior while at lower temperatures a clear saturation is observed in measurements $S1^0$, $S2^0$, and $S3^0$, which correspond to the nonannealed state of the samples and, thus, a higher carrier concentration in the inversion layer. The dotted line in Fig. 3(b) shows the expected mobility values assuming scattering by ionized impurities, $\mu_{ii} \propto T^{-3/2}$. Our experiments show a complex behavior of the mobility which cannot be accounted for by only the reduction of the mobility at lower temperatures as a result of the impurity scattering mechanism, as was previously suggested.³

IV. DISCUSSION

Summarizing the results of the previous section, we have investigated the temperature dependence of the conductivity,

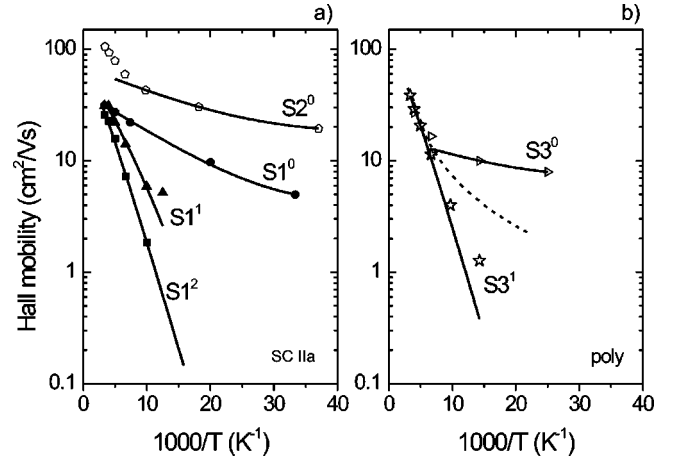


FIG. 3. Temperature dependence of the mobility for the samples in Fig. 1(a). Monocrystalline synthetic type-IIa samples ($S1$ and $S3$). (b) Undoped polycrystalline sample ($S3$). Open and solid symbols correspond to the experimental results. Solid lines correspond to the calculation of the model described in the text. The dashed line represents the expected behavior in the case of the impurity scattering mechanism.

carrier concentration, and Hall mobility in surface conductive diamond samples where 2D transport is expected to occur due to holes accumulated in inversion layers induced at the diamond surface. Whereas the carrier concentration is almost independent of the temperature (as expected for 2D transport in extended states in the absence of localization), both the conductivity and Hall mobility show an exponential temperature dependence in the high-temperature regime, with the activation energy increasing with decreasing carrier concentration. At low temperature and very high carrier concentration, an almost constant Hall mobility and conductivity is observed. For low carrier concentration and low temperatures, the conductivity deviates from the activated behavior, with the activation energy decreasing as the temperature decreases. The results are qualitatively the same for monocrystalline and polycrystalline diamond samples.

As stated in the Introduction, these experimental observations cannot be accounted for by the Anderson-Mott mobility-edge model. The “ideal” Anderson mobility-edge model, modified by Mott,¹⁴ predicts a thermally activated conductivity as a result of disorder-induced localization of carriers. Based on the Anderson model for localization of electrons moving in a system with potential fluctuations associated with microscopic inhomogeneities in the material, Mott showed that electrons near the band edge will be localized, even if the potential fluctuations are not too large.¹⁴ The effect of the potential fluctuations is to smear the sharp edges of the valence and conduction bands: lower states become localized whereas the high energetic states remain delocalized. Mott introduced the concept of the mobility edge E_c , an energy which separates extended states from localized states. Above E_c the wave function of the electrons extend throughout the system, corresponding to a diffuse regime. Below E_c carriers are localized, and they can only move by thermal excitation to extended states or by thermally activated tunneling to another localized state. Thus, if the Fermi energy

(E_F) lies in the localized states ($E_F < E_c$) and the temperature is high enough, conduction occurs by excitation of carriers to the mobility edge, with a conductivity

$$\sigma = \sigma_{\min} e^{-(E_c - E_F)/kT} \quad (1)$$

where σ_{\min} is the 2D minimum metallic conductivity at the mobility edge, with an approximate value of $0.12e^2/\hbar$ ($\cong 3 \times 10^{-5} \Omega^{-1}$), and independent of other parameters such as carrier concentration or Fermi energy position. At very low temperature, when the thermal energy is not sufficient to excite electrons to the extended states, the dominant conductivity mechanism will be thermally activated tunneling between localized states (variable-range hopping), which generates a temperature-conductivity dependence that for a 2D system is¹⁵

$$\sigma = \sigma_0 e^{-(T_0/T)^{1/3}} = \sigma_0 e^{-3(\alpha^2/\pi N kT)^{1/3}} \quad (2)$$

where α is the tunneling exponent (or the inverse of the localization length) and N is the density of localized states at E_F . σ_0 is a parameter that has a weak temperature dependence. On the other hand, metallic conduction in extended states occurs when the Fermi energy lies above the mobility edge.

Therefore, in the high-temperature range (when $kT/q > E_c - E_F$) the “ideal” Anderson-Mott model predicts a temperature-activated conductivity with the activation energy decreasing as the carrier concentration increases. Eventually, the temperature activation disappears and the conductivity becomes metallic. As derived from Eq. (1), the value of the conductivity at $1/T=0$ is a constant independent of the carrier concentration. Concerning the Hall effect, the “ideal” Anderson-Mott model predicts an activated carrier concentration when conduction is dominated by thermal excitation into excited states, while the mobility should show a weak temperature dependence (as expected for scattering mechanisms such as impurity, interface roughness, or phonon scattering). As shown above, none of the predictions of the “ideal” Anderson-Mott model are observed in our experimental results: the minimum metallic conductivity value (calculated as the extrapolation of the conductivity plot in Fig. 1 at $1/T=0$) is not constant, increasing with increasing carrier concentration; the carrier concentration, as measured from Hall experiments, is not activated with temperature; and finally, the Hall mobility is activated with temperature in a very similar way as the conductivity. Thus, our experimental results can be considered as another example of what has been named “nonideal” activated transport in inversion layers with strong localization. Experimental results similar to ours have been previously reported in the literature, and different models, based on long-range potential fluctuations,⁹ hopping transport,⁷ and correlation effects have been proposed to explain the “nonideal” activated transport. Strong correlation between electrons has been suggested to give rise to the correct temperature dependence of conductivity, carrier concentration, and mobility.¹⁰ However, correlation effects are not expected to be important in the temperature regime reported in this paper (from 30 up to 300 K).

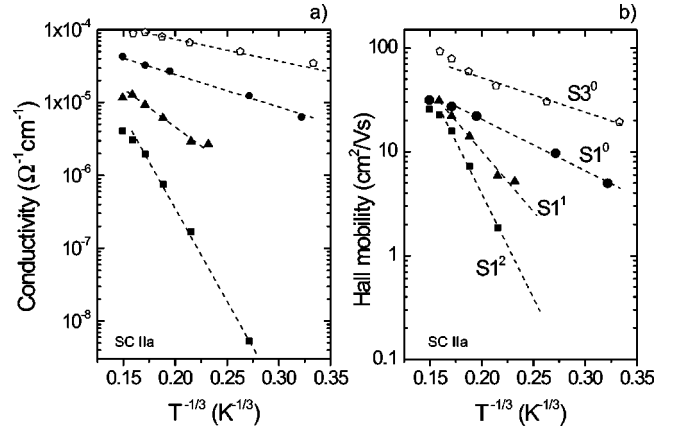


FIG. 4. Analysis of the conductivity and the Hall mobility based on variable-range-hopping transport. (a) Temperature dependence of the conductivity plotted versus $T^{1/3}$ showing a good agreement with Eq. (2). (b) Temperature dependence of the mobility plotted versus $T^{-1/3}$. The slopes of the fits are almost identical for conductivity and Hall mobility.

Hopping transport between localized states was early proposed to explain the conductivity-temperature dependence of “nonideal” activated transport in silicon inversion layers.¹¹ The conductivity of n -channel metal-oxide-semiconductor field-effect-transistor devices was studied in the temperature range $4.2 < T < 77$ K, showing a behavior very similar to that in Fig. 1. Hartstein and Fowler found that the conductivity obeyed a $\ln \sigma \propto T^{-1/3}$ dependence, which was interpreted as indicative of variable-range-hopping transport.¹¹ We have also considered the possibility of variable-range hopping (VRH) transport in the inversion layers at the surface of hydrogen-terminated diamond. Figure 4(a) shows the conductivity versus $T^{-1/3}$, which might indicate a dominant VRH mechanism in the whole temperature range [see Eq. (2)]. However, VRH fails when we consider the measured Hall mobility and carrier concentration. The Hall mobility obeys a temperature dependence which is almost identical to that of the conductivity [Fig. 4(b)]. Variable-range hopping occurs via phonon-assisted tunneling between localized states, so a classical treatment of the Hall effect affecting carriers during hopping is not appropriate. Holstein showed that for multi-hopping processes it is possible to obtain a dependence of the jumping rate on magnetic field.¹⁶ Based on the work of Holstein, Gruenewald *et al.* predicted,¹⁷ in the case of transport in 3D, a temperature dependence of the Hall coefficient and the Hall mobility of the form

$$R_H = R_{H0} e^{(1-\delta)(T_0/T)^{1/4}}, \quad (3)$$

$$\mu_H = \mu_{H0} e^{-\delta(T_0/T)^{1/4}} \quad (4)$$

with $\delta=3/8$. This prediction was later confirmed experimentally.¹⁸ In the case of Eqs. (3) and (4), corresponding to transport in 3D, the exponent of the temperature dependence is $\frac{1}{4}$ compared to the exponent $\frac{1}{3}$ in Eq. (2), which corresponds to transport in 2D.¹⁵ Thus, VRH predicts that both the Hall mobility and Hall carrier concentration ($n = 1/qR_H$) are thermally activated with temperature, obeying

TABLE I. Results of fitting the temperature dependence of the conductivity and the Hall mobility with Eqs. (2) and (4), as expected for variable-range-hopping transport. The value of the coefficient δ is almost 1, in disagreement with the prediction of the 3D VRH model for the Hall effect.

| Sample | $T_{0\sigma}^{1/3}$ (K ^{1/3}) [ln $\sigma \propto -(T_0/T)^{1/3}$] | $\delta T_{0\mu}^{1/3}$ (K ^{1/3}) [ln $\mu_H \propto -\delta(T_0/T)^{1/3}$] | δ |
|-----------------|----------------------------------------------------------------------------------|-------------------------------------------------------------------------------------------|----------|
| S3 ⁰ | 6.49 | 7.43 | 1.14 |
| S1 ⁰ | 10.79 | 10.43 | 0.96 |
| S1 ¹ | 25.92 | 25.74 | 0.99 |
| S1 ² | 58.96 | 48.35 | 0.82 |

Eqs. (3) and (4), respectively. As discussed previously, our results do not show any exponential activation of the Hall carrier concentration with temperature. Figure 4(b) shows the Hall mobility of our samples versus $T^{-1/3}$. Dashed lines in Figs. 4(a) and 4(b) represent best fits to the experimental results of the form $\ln \sigma \propto -(T_0/T)^{1/3}$ and $\ln \mu_H \propto -\delta(T_0/T)^{1/3}$. The results are summarized in Table I, indicating a value of $\delta \sim 1$, in contrast to the prediction of the 3D VRH model.

Based on a model of long-range fluctuations in the oxide charge and the surface potential in silicon inversion layers, Arnold predicted a temperature dependence of the conductivity, Hall mobility, and carrier concentration very similar to those reported in this paper.⁹ Using semiclassical percolation theory, he described the transport of carriers in the strongly localized system, as “a combination of percolation around, scattering from, and thermal emission over random potential barriers.” Potential fluctuations in the silicon surface inversion layer are relatively long-range, giving rise to a macroscopically inhomogeneous transport channel. This means that the bottom of the conduction band (E_C) varies with position, and at $T=0$ “metallic” regions ($E_F > E_C$) coexist with “insulating” regions ($E_F < E_C$). As carriers enter the inversion layer they go to the regions of lower potential, forming “metallic” lakes, which at low enough carrier concentrations are isolated from each other by “insulating” regions. In this situation, conduction occurs by thermal activation of carriers over the barriers separating metallic lakes, giving rise to a thermally activated conductivity. At very low temperatures tunneling through the potential barriers becomes progressively dominant, with the conductivity-temperature dependence obeying Eq. (2), as expected for variable-range-hopping transport. On increasing the number of carriers in the inversion layer, the metallic lakes become larger and the potential barriers separating them become lower. At the percolation threshold, which in a 2D system occurs when the fraction of insulating area (ϵ) equals the fraction of conductive area, continuous percolation paths between the metallic lakes are established for the first time. Activation transport remains above the percolation threshold, especially at higher temperatures when carriers have enough thermal energy to be excited over the residual potential barriers, leading to a reduction of the resistance of long percolating paths. At very low temperatures, when the thermal energy is not enough to overcome the potential barriers, the conductivity should become independent of temperature and, thus, gradually devi-

ate from the exponentially activated behavior. Finally, at very high carrier concentration, when the metallic lakes occupy the majority of the surface, the conductivity becomes independent of temperature. Using the effective medium theory for a 2D binary compound, it is possible to obtain the dependence of the conductivity and Hall mobility on temperature and carrier concentration:⁹

$$\sigma(E) = \frac{1}{2}(1 - 2\epsilon)(\sigma_1 - \sigma_2) + \left[\frac{1}{4}(1 - 2\epsilon)^2(\sigma_1 - \sigma_2)^2 + \sigma_1\sigma_2 \right] \quad (5)$$

where σ_1 and σ_2 are the average conductivity in the metallic regions and the average conductivity in the insulating regions, respectively. Using a rough approximation, the conductivity in the insulating regions can be described by an averaged energy difference between the Fermi energy and the bottom of the conduction band $\langle E_F - E_C \rangle_2$, and thus can be written as

$$\sigma_2 \approx \sigma_1 e^{\langle E_F - E_C \rangle_2 / kT} \quad (6)$$

with σ_1 and $\langle E_F - E_C \rangle_2$ depending on the position of the Fermi level, and thus on the carrier concentration. It should be mentioned that in his original paper Arnold used a more complex description of the conductivity in the insulating regions, by introducing a Gaussian potential distribution to describe the surface potential fluctuations.

Using Eqs. (5) and (6) we have fitted the experimental values of the conductivity plotted in Fig. 1(a) and 1(b), where solid lines represent the results of this fit. Table II summarizes the values of the fitting parameters: the averaged activation energy ($\langle E_F - E_V \rangle_2$), the metallic conductivity (σ_1), and the surface fraction occupied by insulating regions (ϵ). The model described by Eqs. (5) and (6) (solid lines in Fig. 1) reproduces quite reasonably the main characteristics of the experimental results: (i) a decrease of the carrier concentration results in an increase of the activation energy, and (ii) above the percolation threshold a saturation of the conductivity is observed at low temperature, due to the remaining percolation paths. However, below the the percolation threshold (low carrier concentration) and at low temperatures, the model does not describe accurately the temperature dependence. As explained before, at this temperature VRH transport becomes more and more important and it should be taken into account. The dotted lines in Figs. 1(a) and 1(b) are fits to the data using Eq. (2), which describes VRH in 2D transport. The values of the metallic conductivity σ_1 are plotted versus the carrier concentration in Fig. 5(a), showing an increase of the metallic conductivity ($2 \times 10^{-5} - 10^{-4} \Omega^{-1}$) with increasing carrier concentration ($10^{12} - 10^{13} \text{ cm}^{-2}$). As discussed above, the classical Anderson-Mott mobility edge is not able to explain this behavior. Similar experimental results have been previously reported for Si inversion layers, in which it was found that $\sigma_1 \propto n^\beta$, with the exponent β varying between 1 and 2.¹⁰ This behavior was attributed to the increase of screening at higher carrier concentration, which results in lower carrier scattering. However, the exponent $\beta \approx 0.45$ calculated from our results in Fig. 5(a) is lower than 1. Additionally, the holes accumulated at the diamond sur-

TABLE II. Summary of the parameters used for the fit shown in Fig. 1 (conductivity) and Fig. 3 (Hall mobility), based on the model described in the text. $\langle E_F - E_V \rangle_2$ represents an average activation energy, σ_1 the metallic conductivity, μ_1 the metallic mobility, and ε the fraction of surface occupied by insulating regions.

| Sample | Conductivity fit | | | Hall mobility fit | | |
|-----------------|---------------------------------------|---------------------------------|---------------|---------------------------------------|-----------------------------------------|---------------|
| | $\langle E_F - E_V \rangle_2$ (mV) | σ_1 (Ω^{-1}) | ε | $\langle E_F - E_V \rangle_2$ (mV) | μ_1 ($\text{cm}^2/\text{V s}$) | ε |
| S2 ⁰ | 13 | 1.2×10^{-4} | 0.35 | 11.3 | 68 | 0.37 |
| S1 ⁰ | 14 | 5×10^{-5} | 0.45 | 15 | 40.7 | 0.45 |
| S1 ¹ | 28 | 3×10^{-5} | 0.65 | 31 | 75 | 0.65 |
| S1 ² | 45 | 2×10^{-5} | 0.79 | 38 | 90 | 0.79 |
| S3 ⁰ | 12 | 6×10^{-5} | 0.29 | 11.4 | 16.4 | 0.29 |
| S3 ¹ | 44 | 4×10^{-5} | 0.6 | 48 | 122 | 0.6 |

face show a reduced mobility at higher carrier concentration, indicating the surface potential scattering effect.⁸ Figure 6 (open symbols) shows the value of the Hall carrier mobility measured at room temperature for many different samples with carrier concentrations varying between 10^{11} and 10^{13} cm^{-2} . The strong decrease of the carrier mobility with the number of carriers accumulated in the surface channel can be attributed to an increase of surface potential scattering, due to a higher confinement of carriers close to the surface. A large density of charged adsorbates is expected to compensate the holes accumulated in the channel at the diamond surface,² so it is quite reasonable that this very high density of scattering centers gives rise to the main scattering mechanism. Therefore, the variation of the Hall mobility with the carrier concentration shown in Fig. 6 can explain the measured dependence of the metallic conductivity of the form $\sigma_1 \propto n^{0.45}$.

The same procedure as the one employed for the conductivity can be used to fit the Hall mobility results. The Hall effect in disordered materials was initially analyzed using an effective medium theory for 3D systems,¹⁹ and later on for

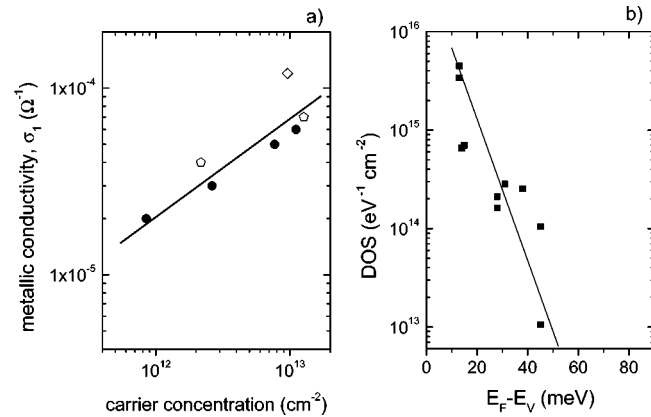


FIG. 5. Relevant parameters deduced from the model described in the text. (a) Metallic conductivity (σ_1) versus carrier concentration. The solid line represents a dependence of the form $\sigma_1 \propto n^{0.45}$. (b) Density of localized states at the diamond surface, calculated from the dependence of the activation energy on the carrier concentration. The solid line is the best fit to the data (solid symbols), assuming an exponential band tail of states.

2D systems.²⁰ It was found that the Hall coefficient of a 2D conductor is insensitive to resistive inclusions until their concentration reaches the percolation threshold ($\varepsilon=0.5$).²⁰ Below the percolation threshold, for $0.75 > \varepsilon > 0.5$, the same is approximately valid depending on the ratio between the resistivity of the conducting and insulating regions. Thus, the effective medium theory predicts a Hall coefficient (R_H) equal to the Hall coefficient of the metallic regions (R_1), which is not temperature dependent. Therefore, the Hall mobility can be calculated as

$$\mu_H(E_F, T) = R_H \sigma \approx R_1(E_F) \sigma(E_F, T) \quad (7)$$

which shows that the Hall mobility should have the same temperature dependence as the conductivity. The experimental results of the Hall mobility shown in Figs. 3(a) and 3(b) have also been fitted using the same approach as for the conductivity. Solid lines in Figs. 3(a) and 3(b) correspond to the results of the fit, whose parameters are summarized in Table II. In this case, the parameter ε was assumed to have the same value as obtained by the fit of the conductivity. Table II confirms that both Hall mobility and conductivity are very well described by the same temperature dependence.

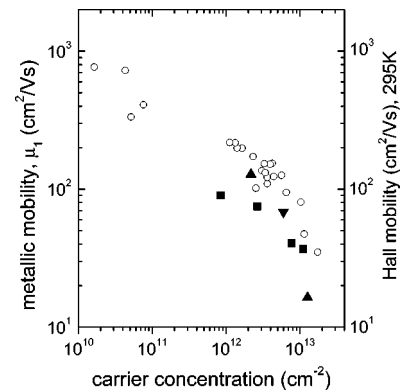


FIG. 6. Calculated values of the metallic mobility (solid symbols) and the effective Hall mobility at room temperature (open symbols) of a set of different samples showing a large variation in carrier concentration. The mobility shows a strong decrease as the carrier concentration increases, suggesting a dominant role of surface scattering.

Similar to the conductivity a decrease of the carrier concentration increases the activation energy of the Hall mobility, and a saturation of the Hall mobility is observed at low temperatures in the case of the highest carrier concentrations. For two of the samples ($S2^0$ and $S3^0$) a significant departure from the prediction of the model is observed at high temperatures, which is a consequence of the decrease of the carrier concentration in these samples. It was shown before that there exists a strong dependence of the Hall mobility on carrier concentration (see Fig. 6). In the temperature range where the measured Hall mobility of $S2^0$ and $S3^0$ shows a clear deviation from a simple thermal activation, the carrier concentration is not constant but decreases with increasing temperature. The decrease of the carrier concentration results in an increase of the mobility. From the fit of the Hall mobility, it is also possible to obtain information about the value of the mobility of carriers in the metallic regions, μ_1 in Table II. Solid symbols in Fig. 6 represent the values of the metallic Hall mobility, showing a good agreement with the room-temperature Hall mobility (open symbols) of a set of samples with different carrier concentration. It is clear that the metallic Hall mobility also decreases with increasing carrier concentration, which can be attributed to the effect of surface potential scattering.

As described previously, the average activation energy (for both mobility and conductivity) decreases as the number of accumulated holes increases. The density of localized states at the Fermi energy can be estimated from the variation of the activation energy versus the carrier concentration,

$$N(E_F) = - \frac{\Delta n}{\Delta \langle E_F - E_V \rangle_2}. \quad (8)$$

Figure 5(b) shows the estimated density of localized states at the position of the Fermi level, with the solid line in Fig. 5(b) representing the best fit to a band tail with an exponential distribution of localized states. The density of states at the edge of the valence band can be estimated from the extrapolation of the straight line in Fig. 5(b), which gives a value $N(E_F = E_V) = 3 \times 10^{16} \text{ eV}^{-1} \text{ cm}^{-2}$. The density of states in the unperturbed band, N_0 , is given by $N_0 = m_{2D} / \pi \hbar^2$, where m_{2D} is the effective mass of holes in the 2D inversion layer. To the best of our knowledge, m_{2D} has not been reported for holes in the hydrogen-induced surface inversion layer, so we will use the bulk values of the effective mass for heavy holes ($m_{hh} = 1.08m_0$), light holes ($m_{lh} = 0.36m_0$), and split-off holes ($m_{soh} = 0.15m_0$).²¹ Then, the value of the total density of states (including the hh, lh, and soh bands) in the unperturbed band has a value of $N_0 \approx 8 \times 10^{14} \text{ eV}^{-1} \text{ cm}^{-2}$, which is more than one order of magnitude smaller than the density of localized states. Thus, it follows that the origin of the localized states should rather be attributed to the presence of surface states. Nebel *et al.* also have reported a very high density of surface states, in the range $(1-5) \times 10^{16} \text{ eV}^{-1} \text{ cm}^{-2}$.³

The values of the fraction of the diamond surface (ϵ) occupied by insulating regions have been found to be quite

high. However, as has been shown by Arnold,²² if the potential fluctuations are not random but spatially correlated (for instance, clustering along certain directions), then Eq. (5) has a different form. The effect of the correlations is, thus, to decrease the value of ϵ at any given carrier concentration. An “ordered” arrangement of surface adsorbates will certainly result in spatially correlated potential fluctuations at the surface, resulting in a reduction of ϵ .

V. CONCLUSIONS

The electronic transport properties of holes in 2D inversion layers induced at the surface of hydrogenated diamond samples have been studied in the temperature range 30–300 K. The conductivity and Hall mobility have been studied as a function of temperature and carrier concentration. Our experimental results show a carrier concentration with a weak temperature dependence, resembling the behavior of 2D metallic transport. At high temperatures, the conductivity and Hall mobility show a thermally activated behavior, with almost identical activation energies. The activation energy increases as the number of holes accumulated in the surface channel is reduced. With high carrier concentration and at low temperatures both mobility and conductivity saturate, departing from the simple exponential dependence. We have argued that this result cannot be explained by the classical Anderson-Mott mobility-edge model for transport in inversion layers with disorder-induced localization. Instead, a model originally proposed by Arnold, and based on long-range potential fluctuations, has been used to fit the experimental results with very good agreement. It is suggested that macroscopic potential fluctuations (in contrast to the microscopic potential fluctuations in the Anderson-Mott model) at the diamond surface, probably caused by the presence of charged adsorbates or by an incomplete hydrogen termination, give rise to a situation in which metallic and insulating regions coexist. The insulating regions act as potential barriers between the metallic regions, which gives rise to the reported activated transport. Increasing the number of carriers reduces the potential barrier height, with a corresponding reduction of the average activation energy. The model uses percolation theory to evaluate the contribution of each region to the measured conductivity and Hall mobility. The experimental results were fitted using three parameters: the average potential barrier in the insulating regions, the metallic conductivity (or metallic mobility), and the fraction of surface occupied by insulating regions. The metallic conductivity increases with increasing carrier concentration (in contrast to the prediction of the Anderson-Mott model). However, the metallic mobility decreases with increasing carrier concentration, which has been explained as a result of the surface scattering. From the variation of the activation energy with carrier concentration, the density of localized states at the edge of the valence band in the surface has been estimated to about $3 \times 10^{16} \text{ eV}^{-1} \text{ cm}^{-2}$, which is much higher than the density of states in the bulk unperturbed band.

- ¹R. I. S. Gi, K. Tashiro, S. Tanaka, T. Fujisawa, H. Kimura, T. Kurosu, and M. Iida, *Jpn. J. Appl. Phys., Part 1* **38**, 3492 (1999).
- ²F. Maier, M. Riedel, B. Mantel, J. Ristein, and L. Ley, *Phys. Rev. Lett.* **85**, 3472 (2000).
- ³C. E. Nebel, C. Sauerer, F. Ertl, M. Stutzmann, C. F. O. Graeff, P. Bergonzo, O. A. Williams, and R. Jackman, *Appl. Phys. Lett.* **79**, 4541 (2001).
- ⁴H. J. Looi, R. B. Jackman, and J. S. Foord, *Appl. Phys. Lett.* **72**, 353 (1999).
- ⁵O. A. Williams, R. B. Jackman, C. Nebel, and J. S. Foord, *Semicond. Sci. Technol.* **18**, S77 (2003).
- ⁶E. Arnold, *Appl. Phys. Lett.* **25**, 705 (1974).
- ⁷S. J. Allen, D. C. Tsui, and F. DeRosa, *Phys. Rev. Lett.* **35**, 1359 (1975).
- ⁸T. Ando, A. B. Fowler, and F. Stern, *Rev. Mod. Phys.* **54**, 437 (1982).
- ⁹E. Arnold, *Surf. Sci.* **58**, 60 (1976).
- ¹⁰C. J. Adkins, *Philos. Mag. B* **38**, 535 (1978).
- ¹¹A. Hartstein and A. B. Fowler, *J. Phys. C* **8**, L249 (1975).
- ¹²J. B. Cui, J. Ristein, and L. Ley, *Phys. Rev. B* **59**, 5847 (1999).
- ¹³J. A. Garrido, C. E. Nebel, R. Todt, M.-C. Amann, O. A. Williams, R. Jackman, M. Nešládek, and M. Stutzmann, *Phys. Status Solidi A* **199**, 56 (2003).
- ¹⁴N. F. Mott, *Philos. Mag.* **13**, 689 (1966).
- ¹⁵N. F. Mott, M. Pepper, S. Pollit, R. H. Wallis, and C. J. Adkins, *Proc. R. Soc. London, Ser. A* **345**, 169 (1975).
- ¹⁶T. Holstein, *Phys. Rev.* **124**, 1329 (1961).
- ¹⁷M. Gruenewald, H. Mueller, P. Thomas, and D. Wuertz, *Solid State Commun.* **38**, 1011 (1981).
- ¹⁸A. Roy, M. Levy, X. M. Guo, M. P. Sarachik, R. Ledesma, and L. L. Isaacs, *Phys. Rev. B* **39**, 10185 (1989).
- ¹⁹M. H. Cohen and J. Jortner, *Phys. Rev. Lett.* **30**, 696 (1973).
- ²⁰C. J. Adkins, *J. Phys. C* **12**, 3389 (1979).
- ²¹L. Reggiani, D. Waechter, and S. Zukotynski, *Phys. Rev. B* **28**, 3550 (1983).
- ²²E. Arnold, *Phys. Rev. B* **17**, 4111 (1978).